Communication

A Micropillar Compression Methodology for Ductile Damage Quantification

C.C. TASAN, J.P.M. HOEFNAGELS, and M.G.D. GEERS

Microstructural damage evolution is reported to influence significantly the failures of new high-strength alloys. Its accurate quantification is, therefore, critical for (1) microstructure optimization and (2) continuum damage models to predict failures of these materials. As existing methodologies do not fulfill the requirements, there is an active search for an accurate damage quantification methodology. In this article, a new, micropillar, compression-based methodology is presented, whereby damage evolution can be quantified successfully through the degradation of the modulus caused by previous deformation.

DOI: 10.1007/s11661-011-1021-4

Recently, immense efforts have been made to understand the microstructural damage mechanisms (*e.g.,* microcracks and microvoids) observed in the new high-strength metals (*e.g.,* dual-phase steels, advanced aluminum alloys, *etc.*) to understand and predict the complex material behavior and failure of these advanced materials. Next to these qualitative analysis efforts, there has also been significant interest in the quantitative analysis of the damage activity, not only to allow the comparative analysis (of the damage-sensitivity) required to optimize these new microstructures but also to predict their complex mechanical behavior through continuum damage models. However, the accurate quantification of ductile damage is a significant challenge and (contrary to popular belief) not trivially possible using the existing *morphology based* experimental techniques (*e.g.,* electron micrography, X-ray microtomography, and highly sensitive mass and volume measurements).[1–3] These methodologies probe a geometric damage parameter based on either void area fraction, void volume fraction, or porosity density, which do allow for a qualitative analysis of damage mechanisms to optimize damage-sensitive microstructures. However, the geometric damage parameter does not probe directly how the deformation mechanics is affected by the amount of damage, damage morphology, or interaction effects.[4,5] Therefore, a mechanical property-based experimental technique is needed that directly probes the mechanical influence of deformation-induced damage (rather than its geometry), with sufficiently high spatial resolution to capture high strain and damage gradients. The indentation-based methodology,[6] where deformation-induced hardness degradation is probed to quantify a mechanical damage parameter D, has received considerable attention as the most promising mechanical approach to fulfill these requirements.[1,7–9] This methodology was extended by Guelorget *et al.*[9] to probe the damage parameter from the degradation of the indentation modulus (obtained via the Oliver-Pharr methodology[10]) through

$$D^{\mathrm{E}} = 1 - \frac{E^{\mathrm{D}}}{E} \qquad [1]$$

where E^{D} is the indentation modulus of the damaged material and E is the indentation modulus in the undeformed state. This extension is significant as degradation of the modulus connects directly to the damage definition employed in continuum damage models.*

*The fact that the indentation modulus may differ from the real material modulus is unimportant as only the change in modulus is related to the damage.

However, it was shown by the authors recently that the indentation-based approach is intrinsically deficient because of plasticity-induced microstructural effects (indentation pile-up, strain hardening, grain shape change, texture formation, *etc.*), which mask the degradation of hardness completely and also cause severe artifacts in the modulus.[11] Consequently, alternative mechanical testing strategies that surpass this challenge are needed for (high spatial resolution) quantification of ductile damage.

The authors have presented such an alternative approach recently, whereby the undesired plasticity effects are removed by partial homogenization heat treatments (which leaves the voids unaffected), allowing the damage effect to be captured through indentation experiments.[12] Although this heat treatment-assisted indentation (HTI) methodology works successfully, a more practical alternative approach would be required for situations in which more rapid solutions would be beneficial (*e.g.,* for industrial applications) or for critical applications where the obtained damage evolution law needs to be double checked with an alternative approach. Therefore in this article, a second, easier to implement mechanical-property-based damage measurement technique is presented, in which the plasticity effects are avoided (instead of being removed) by probing only the elastic response of the damaged metal. This is achieved by an innovative methodology based on compression tests on micropillars, which quantifies

C.C. TASAN, Postdoctoral Researcher, is with the Materials Innovation Institute (M2i), P.O. Box 5008, 2600 GA Delft, The Netherlands, and is also with the Department of Microstructure Physics and Alloy Design, Max-Planck-Institut für Eisenforschung GmbH, Max-Planck-Str. 1, 40237 Düsseldorf, Germany. J.P.M. HOEFNAGELS, Assistant Professor, and M.G.D. GEERS, Full Professor, are with the Department of Mechanical Engineering, Eindhoven University of Technology, Den Dolech 2, 5612 AZ Eindhoven, The Netherlands. Contact e-mail: j.p.m.hoefnagels@tue.nl
Manuscript submitted July 17, 2011.
Article published online December 14, 2011

damage-induced softening through the degradation of the elastic modulus of compression. The forementioned microplasticity-induced problems are circumvent with the developed methodology because the modulus of compression is measured on micropillars with a flat punch (instead of the sharp indenter of the original indentation methodology, which inherently induces plasticity around the indenter tip) and the load levels are kept well below the point of yielding, thereby minimizing localized plasticity.

The new methodology will be demonstrated on a commonly used industrial sheet metal grade: dual phase 600 (DP) steel (the mechanical behavior of which is shown in Figure 1(a) and is verified by comparison with the previously mentioned HTI technique on the same steel). Preliminary analyses of the deformed microstructures of this material revealed the active damage mechanisms to be severe plastic straining near martensite–ferrite phase boundaries (Figure 1(b)) and martensite cracking (Figure 1(c)). The activity of these mechanisms at different positions in the specimens were analyzed quantitatively using a gray value thresholding-based image postprocessing program that registers damage incidents over the full cross section of deformed DP600 samples (prior to the manufacturing of the pillars). This statistical analysis showed that the phase boundary damage mechanism is the more active mechanism for the employed DP steel throughout the whole deformation range (*i.e.,* also after the point of strain localization), such that for every one martensite cracking incident, roughly nine phase boundary damage incidents were identified consistently in different regions of the specimens deformed to different levels (Figure 1(a)).

To carry out the tests shown in Figure 1, three tensile specimens (Figure 2(a)) of DP steel are cut using electrodischarge machining (EDM), painted with speckle patterns and tested to the point of fracture using a microtensile stage (Figure 2(b)), whereas the local equivalent strains are calculated from a digital image correlation analysis. The deformed samples are cut into four pieces each along their central axis using wire EDM (with a diameter of 0.1 mm) (Figure 2(c)). Pillars of square cross section (*i.e.,* 0.2×0.2 mm^2) are produced at the cross sections of the tensile specimens, with two perpendicular sets of 0.4-mm-deep parallel wire EDM cuts (Figure 2(d)).**

**Focused ion beam milling, which has received significant attention recently to study the size dependent plasticity,[13,14] is not an option for the current purpose because of the total volume of material that needs to be removed.

The size of the pillars ($0.2 \times 0.2 \times 0.4$ mm^3) are selected such that a representative material volume that contains hundreds of grains is probed, whereas sufficient spatial resolution is maintained to capture high strain and damage gradients.

Load-controlled compression tests are carried out using a microindenter (CSM Instruments, Needham, MA) with a flat punch of 0.35 mm diameter. Scanning electron microscopy and confocal microscopy analyses are carried out to verify that the punch is perfectly flat and clean of contamination, which are critical in avoiding plasticity (Figure 3). From each tested micropillar, load *vs* displacement data are obtained (Figure 3), which are used to extract the elastic compression modulus. The loading–unloading scheme is designed especially to minimize the influence of surface plasticity on the modulus measurement (Figure 3): The micropillars are compressed first up to 2N load level, which corresponds to approximately half of the material yield strength. During this pretreatment, no plasticity is induced in the bulk while the surface roughness is plastically deformed and hardened. The micropillars are unloaded subsequently to 0.4N, and then they are

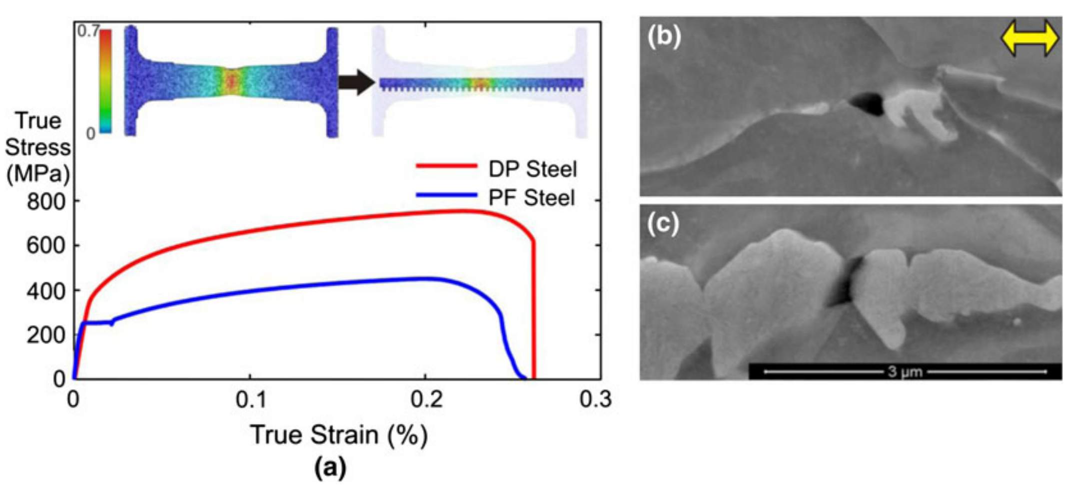

Fig. 1—(*a*) Uniaxial tension tests results of the tested dual-phase steel and the pearlitic-ferritic steel employed in this work. Digital image correlation analysis is used to measure local strain distribution maps and determine strain levels corresponding to different pillars, as shown in the inset image. Example SEM images of the (*b*) damage mechanism at the martensite–ferrite phase boundary and (*c*) damage mechanism caused by martensite cracking are also shown. Deformation test direction (yellow arrow) and the micron-bar are for both SEM images (Color figure online).

reloaded and unloaded three times between the 0.4N and 1N. During this treatment, no plasticity is triggered in the bulk or in the surface region. The modulus is calculated on the higher 60 pct portion of the unloading from 1N. The same procedure is repeated on pillars on different locations on the specimen, each location corresponding to a particular predeformation level, ε, known from the local strain field measurement. For the same strain level, the same modulus is found consistently that agrees within experimental uncertainty. Note that the damage incident registration analysis mentioned previously also verified that different regions of the same strain level are in agreement within a statistical uncertainty of 15 pct in the number of damage incidents per surface area.†

†The pillar compression test probes material volume rather than surface area, which decreases this statistical uncertainty even more.

With increasing predeformation, the measured unloading slope (*i.e.,* modulus) decreases as a result of the increasing damage in the microstructure (Figure 3). This decrease in the obtained modulus data is used to calculate the damage parameter D^E (using Eq. [1]), where the modulus in the undeformed state is measured on the pillars outside the specimen gauge section (behind the clamps of the tensile tester). Finally, D^E is coupled to the measured local strains to reveal its evolution with deformation.

The deformation-induced evolution of the compressive modulus of DP steel is shown in the upper section of Figure 4 (with filled upward triangle data points). It is observed that the modulus is constant at low strain levels and then begins to degrade at an increasing rate, and finally it reaches a minimum after strain localization ($\varepsilon > \sim 0.5$). Although this trend was expected, it is still striking to observe because such a trend was not captured with the original indentation-based methodology performed on exactly the same material (caused by the plasticity-induced microstructural effect explained in the introduction).[11] The overall trend and the total amount of decrease in modulus reveal a realistic damage evolution behavior as shown in the lower part of Figure 4 (with the filled downward triangle data points). The damage value stays constant within experimental accuracy at ~0 pct up to a critical strain level ($\varepsilon = \sim 0.24$), then it increases approximately linearly to 5 pct, and finally grows rapidly to ~20 pct at the onset of fracture. Note that these high levels of final damage values are in accordance with the microstructural observations (Figure 2(e)).

Although this result is conclusive on the capability of the current methodology in capturing the damage-induced softening, two sets of additional analyses are carried out to verify the accuracy of the obtained results.

It is verified first that the trend in the measured modulus is indeed caused solely by the evolution of damage in the material and is not affected by other microstructural or mechanical heterogeneities (*e.g.,* texture evolution, residual stress buildup, *etc.*) caused by previous deformation. Such effects are detrimental for the accurate quantification of damage, as shown previously by the authors for the original indentation

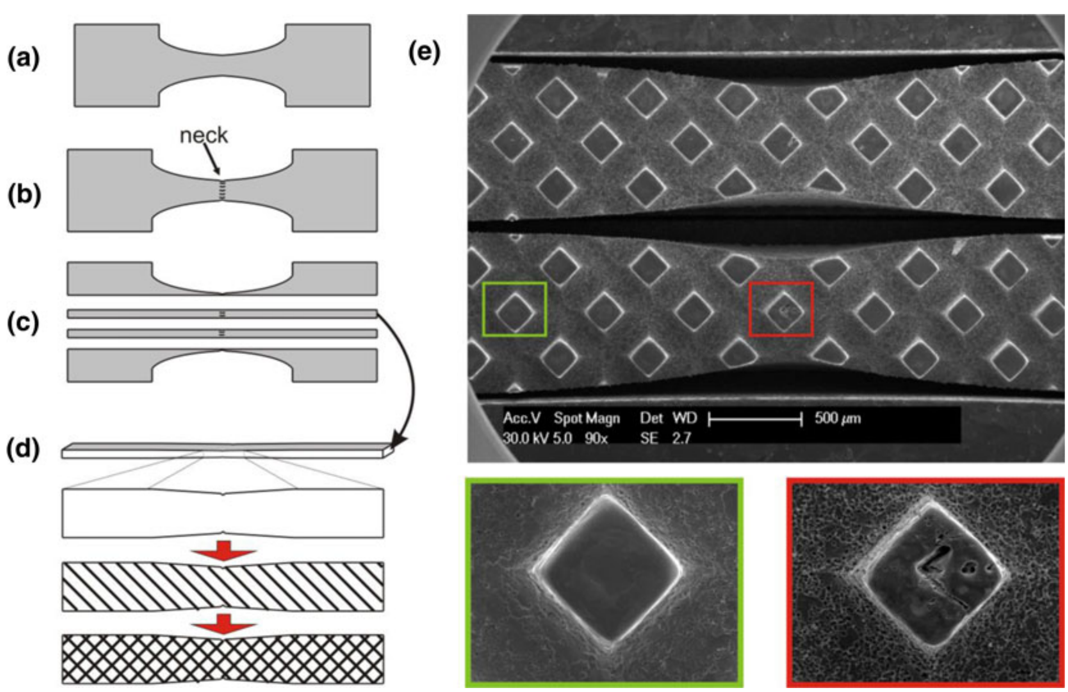

Fig. 2—The experimental methodology starts with tensile specimens (*a*) that are tested to the point of fracture. (*b*) The deformed samples are cut into four pieces along their central axis with three wire EDM cuts (*c*), followed by two perpendicular sets of wire EDM cuts on the cross section at 45 deg with the tensile direction (*d*) to produce the field of micropillars shown in (*e*). Note the microvoids visible at the top of pillars located at highly deformed regions around the neck.

methodology.[11] Although it is virtually impossible to separate the influence of such heterogeneities on the compression modulus, it is possible with the previously mentioned partial homogenization heat treatment to remove such effects altogether, whereas the damage is left unaffected. Therefore, this heat treatment (for details see Reference 12) is applied to the deformed martensitic-ferritic DP steel samples with the micropillars, resulting in a pearlitic-ferritic (PF) matrix microstructure surrounding the existing damage. Note that although the resulting homogeneous matrix microstructure is different from the original microstructure (Figure 1 shows the uniaxial tension behavior of the previously undeformed, as-heat-treated PF steel), finite-element simulations have shown that this has no significant effect on the measured damage values.[12] Follow-up elastic compression tests (carried out in the same manner) show no significant changes in the relative decrease in modulus after the heat treatment (the unfilled star-shaped data points are shown in the upper section of Figure 4), revealing that the influence of other microstructural changes on the degradation of elastic modulus is at least smaller than the experimental uncertainty.

Second, to verify the overall accuracy of the damage evolution data obtained, the damage evolution in the same material is also quantified using an alternative measurement, the HTI methodology,[12] which provides two sets of damage evolution data (*i.e.,* indentation-hardness based and indentation-modulus based) shown with the unfilled circle and square data points in the lower section of Figure 4. Clearly, the comparison verifies the accuracy of the micropillar approach, revealing the same damage initiation point and the damage accumulation profile up to the onset of fracture. Beyond the point of fracture, the strain measurement uncertainty obstructs a good comparison between the two methodologies.

Finally, some discussion is presented on how the presented precision and accuracy is achieved by avoiding a significant influence of the possible manufacturing errors during the EDM process (*e.g.,* small variations in pillar dimensions and EDM-influenced surface layer). Indeed, high manufacturing accuracy is important to obtain accurate *absolute* compression modulus values from micropillar experiments. However, in the proposed methodology, the measured damage value depends only on the decrease of the modulus, thus on the *relative* measurement of the modulus, which is independent of the exact pillar dimensions as long as the pillars are produced with high precision using the same EDM process conditions and with the same target micropillar dimensions. In the same way, any change of material properties resulting from a EDM-induced heat-affected outer layer of the micropillars has negligible effect on the measured damage value because (1) the measured damage value is nearly independent of material properties as demonstrated in Reference 12 and shown experimentally in Figure 4; (2) all micropillars were subjected to the same EDM process, thus the EDM influence on the modulus is the same; and (3) the relative volume fraction of the heat-affected zone compared with the total micropillar is small. However, it should be noted as a general limitation of the methodology that the EDM-based manufacturing process limits clearly the possibility of carrying out stop-test types of analyses. This point may be of importance in case of a material in which damage evolution follows different paths at different positions of the specimen. On the other hand, the proposed pillar compression test is suited ideally to measure such differences as it probes the damage state locally at each pillar. One is then required only to carry

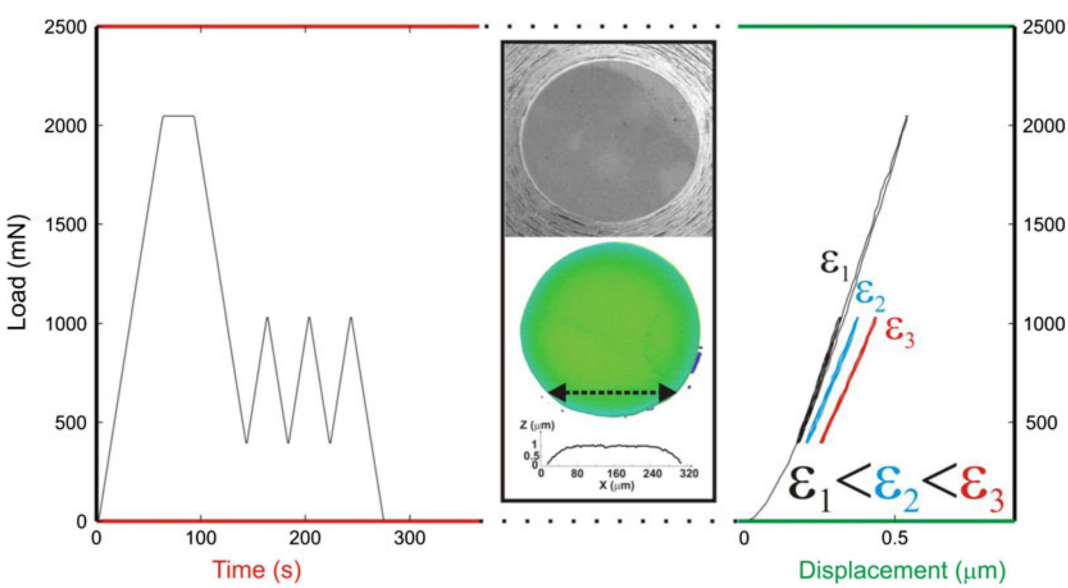

Fig. 3—The loading sequence for the compression tests for the DP steel (left); resulting load *vs* displacement curves (right). Increasing predeformation, ε, creates a drop in slopes of the unloading curves. Note that the first part of the blue and red force displacement data are removed curves is not shown for clarity. Also shown in the inset is the surface analysis of the flat punch: SEM image at the (top), color map of surface topography (middle), and the shown profile (bottom) (Color figure online).

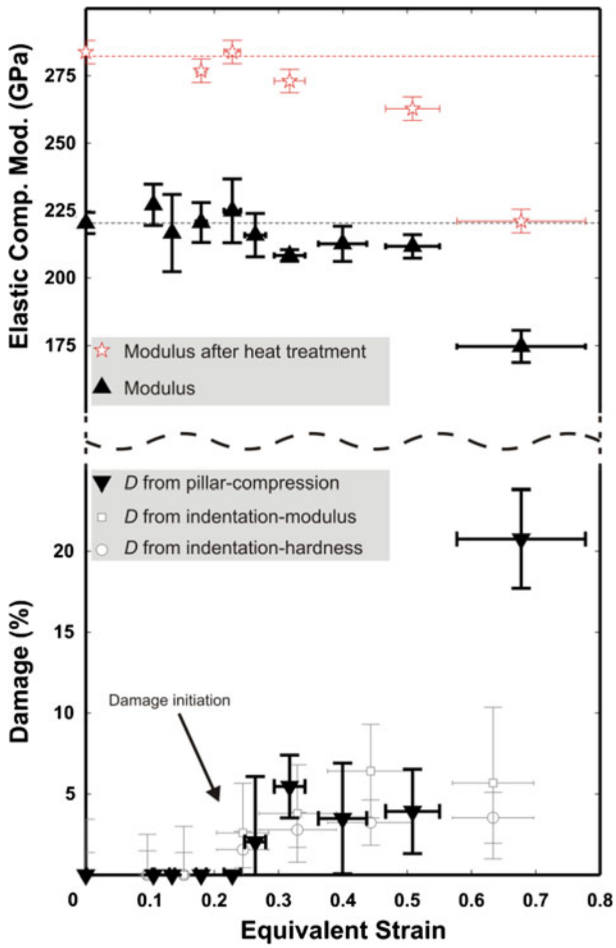

Fig. 4—Compression modulus (above) and damage (below) evolution in DP steel. The reference modulus value at zero strain is shown with straight dashed lines. The vertical error bars represent the standard deviation of the mean. Compression modulus measurements after partial-homogenization heat treatment are shown with the red star-shaped data points. Damage evolution in the same material is also quantified with the HTI methodology, which is shown with gray data points (Color figure online).

out deformation tests to different global strain levels and create pillars for each test to quantify the damage evolution.

To conclude, a promising damage quantification strategy is proposed, whereby the reported challenges with existing indentation-based damage quantification methodology are overcome. This is achieved by a carefully designed damage measurement concept relying on flat punch elastic compression tests on electrodischarge machined micropillars. By keeping the deformation of the pillars in the elastic regime, plasticity effects masking the damage influence in the indentation-based damage quantification methodology are avoided. The evolution of the elastic damage parameter is calculated successfully from the measured degradation of the elastic compression modulus. As mentioned, the use of elastic modulus for damage quantification has the additional advantage of a direct connection to the damage parameter definition in continuum damage models. Compression tests on partially homogenized samples confirmed that the influence of other deformation induced microstructural heterogeneities is negligible with respect to the measured damage influence. The accuracy of the obtained damage parameter has been compared with an alternative mechanical damage quantification methodology as a final verification, proving that the proposed methodology can be used to provide the required material-specific damage evolution parameters for continuum damage models. Ongoing work is concentrated on improving the methodology both regarding the experimental precision and, more importantly, regarding accurate quantification of the high damage gradients in the post-strain localization regime. Whereas increasing precision can be achieved relatively easily by increasing the number of specimens or measurement points, measurements in the post-necking regime is more challenging. The results here demonstrate that a damage level up to a level of 10 to 20 pct can be measured successfully; however, continuum damage models require the full evolution of damage to the point of fracture ($D = 100$ pct). This task is difficult for the case of uniaxial tension considered in this study since methods to carry out accurate quantification of the high damage gradients in the poststrain localization regime is extremely challenging. A promising strategy for future work could be modifying the developed methodology to probe damage evolution in other deformation modes (*e.g.,* bending) where deformation is more constrained and high strain gradients caused by localization are avoided.

This research was carried out under project number MC2.05205 in the framework of the Research Program of the Materials innovation institute M2i (www.m2i.nl), which is the former Netherlands Institute for Metals Research. The contribution of Marc van Maris is also gratefully acknowledged.

REFERENCES

1. M. Alves: *Mech. Based Des. Struc.*, 2001, vol. 29, pp. 451–76.
2. E. Maire, O. Bouaziz, M. Di Michiel, and C. Verdu: *Acta Mater.*, 2008, vol. 56, pp. 4954–64.
3. J.P.M. Hoefnagels, C.C. Tasan, and M.G.D. Geers: *Proc. 7th Euromech Solid Mechanics Conf.*, Lisbon, Portugal, 2009.
4. S. Jansson and U. Stigh: *J. Appl. Mech.*, 1985, vol. 52, pp. 609–14.
5. U. Stigh: *J. Appl. Mech.*, 1986, vol. 53, pp. 485–90.
6. J. Lemaitre and J. Dufailly: *Eng. Fract. Mech.*, 1987, vol. 28, pp. 643–61.
7. G. Arnold, O. Hubert, M. Dutko, and R. Billardon: *Int. J. Form. Processes*, 2002, vol. 5, pp. 163–73.
8. A. Mkaddem, F. Gassara, and R. Hambli: *J. Mater. Process. Technol.*, 2006, vol. 178, pp. 111–18.

9. B. Guelorget, M. Francois, and J. Lu: *Mater. Lett.*, 2007, vol. 61, pp. 34–36.
10. W.C. Oliver and G.M. Pharr: *J. Mater. Res.*, 1992, vol. 7, pp. 1564–83.
11. C.C. Tasan, J.P.M. Hoefnagels, and M.G.D. Geers: *Acta Mater.*, 2009, vol. 57, pp. 4957–66.
12. C.C. Tasan, J.P.M. Hoefnagels, and M.G.D. Geers: *Scripta Mater.*, 2010, vol. 63, pp. 316–19.
13. M.D. Uchic, D.M. Dimiduk, J.N. Florando, and W.D. Nix: *Science*, 2004, vol. 305, pp. 986–89.
14. J.R. Greer, W.C. Oliver, and W.D. Nix: *Acta Mater.*, 2005, vol. 53, pp. 1821–30.